# STUDY OF VOLTAGE INSTABILITY IN POWER SYSTEMS USING CATASTROPHE THEORY

**G.A. MAHMOUD, M.Sc., Ph.D, M.I.E.E.E**
**Suez Canal University, Elect. Eng. Dept., Port-said, EGYPT.**

## دراسة عدم اتزان الجهد فى نظم القوى الكهربية مستخدما نظرية النكبة

الخلاصة :

تعتبر دراسة الاتزان فى نظم القوى الكهربية من الموضوعات التى تزداد اهمية فى الوقت الحاضر. لقد تناولت كثير من البحوث والمراجع هذه الدراسة مستخدمة زاوية الحمل كمقياس فى دراسة الاتزان الديناميكى لنظم القوى الكهربية مستخدمة نظرية النكبة فى الحالة المستقرة والعابرة.

تم فى هذا البحث ادخال اسلوب جديد لدراسة الاتزان فى نظم القوى الكهربية آخذا فى الاعتبار الجهد كاحد المقاييس للاتزان مستخدما نظرية النكبة. لقد تم وصف سلوك نظام القوى المقترح دراسته فى هذا البحث كسلوك نموذج من النماذج السبع المعروفة فى نظرية النكبة.

وتتلخص الاضافات فى هذا البحث فيما يلى:

١ - هذه الدراسة أثبتت امكانية أخذ الجهد كاحد المقاييس فى دراسة الاتزان فى نظم القوى الكهربية.

٢ - أثبتت هذه الدراسة امكانية تطبيق نظرية النكبة فى دراسة الاتزان لنظم القوى الكهربية مستخدما الجهد كاحد المقاييس للاتزان كما تم تطبيقها سابقا مستخدمه زاوية الحمل.

٣ - استنبطت من هذه الدراسة باستخدام المعادلات المستنتجة من نظرية النكبة معادلة اقصى حمل يمكن أن يحمل به النظام الكهربى دون أن يفقد اتزانه. كما تم دراسة تاثير التعويض على التوازى لزيادة حدود التحميل المختلفة.

**Abstract:** Catastrophe theory is a mathematical technique for the qualitative analysis of system equations, defining the jump phenomena and sudden changes caused by smooth changes in the system parameters. This theory has been applied previously to the study of steady state stability of power systems. This paper presents a new technique in the area of power system stability studies to describe steady-state voltage stability in terms of one of the catastrophe manifolds to which the power system can be fitted.

E. 14 G.A.MAHMOUD. M.Sc.Ph.D,M.I.E.E.E

## 1- INTRODUCTION

Steady - state voltage stability in a power system has become increasingly important in recent years.It indicates the capability of the power system to maintain the load voltage within a specified region in steady - state conditions. Todays electric power systems are highly interconnected and the problem of maintaining voltage tolerances at various locations in the transmission network becomes more complex. If the generation facilities are adjacent to load centers, the real and reactive power can be supplied by the generating units. However, in many cases the generation facilities are located long distance from the loads and with this comes the need for compensation of voltage drop along the transmission line and for provision of voltage support at the load areas for both normal and abnormal conditions.

Reactive power problems arise in power systems under a variety of conditions [1]. For lightly loaded systems, too much reactive power may be injected into the network by shunt elements resulting in overly high voltages at the voltage uncontrolled buses. Alternatively under heavy load conditions there may be insufficient injected reactive power causing the voltage drop.

Collapse (or instability) in the system voltage may be occurred as a result of the gradual increase in the system load. In some cases, heavily loaded power systems, particularly when the system configuration comprises long transmission lines, the voltage drop caused by the dropping of a generator or transmission line cannot be recovered even if the static capacitors at load ends are switched on [2]. This sort of abnormal voltage drop is called transient voltage instability or transient voltage collapse phenomena. The load corresponding to this collapse is called critical load. So this phenomena can be put into the framework of the elementary catastrophes. The aim is to verify that the instability corresponds to voltage rather than angle.

Catastrophe theory has been applied to the study of steady state and transient synchronous stability of power system [3-5]. The analysis was with respect to angle instability. But the instabiiity may be manifested in many different ways, depending upon the characteristics and configuration of the system and also on its operating mode [6]. For example, in some cases in which steady - state voltage instability has been approached with no immediate prospect of angle or synchronous instability. This particularly true if generation is away from the load center. This aspect is analytically verified in this paper for two nodes system.

## 2- Catastrophe theory

Some physical system in nature can be exposed to sudden changes arising from smooth variations in the situation [7]. These sudden changes (or jump phenomena) can be analyzed by the catastrophe theory to identify how the equilibrium of the system is changed as the control parameters change. This theory applies most directly to systems which in a range of situations, seek at each moment to minimize a certain function such as the potential or energy function [8].

Consider a gradient dynamical system whose behavior is usually smeoth, but sometimes (or in some places) exhibits discontinuities. Catastrophe theory tries to deal with the properties of these discontinuities. The system can be specified by a potential function V with n-state variables $(x_1, x_2, \ldots, x_n)$ and under the control of m-independent variables $(u_1, u_2, \ldots, u_m)$. The number of different discontinuities that can occur depends not upon the number of state variables but on the number of control variables [9,10]. According to the number of state variables ($n \leq 2$) and the number of control parameters ($m \leq 4$), the catastrophe manifold is determined as one of the seven elementary catastrophes.

The set of all equilibria of the potential function V is given by

$$\frac{\partial V}{\partial x_i} = 0 \qquad i = 1,2,\ldots,n \qquad (1)$$

Define m-dimensional equilibrium surface in the (n+m)-dimensional space. Since the potential depends on control parameters, the Hessian of V and its eigenvalues depend on these control parameters. For certain values of control parameters, one or more of these eigenvalues may assume the value zero.

When this happens, the Hessian,

$$\det [V_{ij}] = 0 \qquad (2)$$

and the system state variables are called nonisolated, degenerate variables. The number of different kinds of catastrophes which can occur depends on these variables.

If the rank of Hessian is n-l for some l>0 (l corresponds to the number of zero eigenvalues), the original potential

function can be split into two parts. This is called splitting lemma [10], because it allows us to split the variables into two parts: part involved in structural stability called non-degenerate associated with the non-vanishing eigenvalues, and the others involved in instability associated with vanishing eigenvalues.

The system potential function V can be written in the catastrophe canonical form .

$$V = Cat(l,m)+\sum_{j=l+1}^{n} \lambda_j \, y_j^2 \qquad (3)$$

where,

| | |
|---|---|
| Cat(l,m) | is the catastrophe function |
| $\lambda_j$ | is the number of non-zero eigenvalues |
| $y_j$ | is the coordinates associated with non-vanishing eigenvalues. |

The catastrophe function gives the qualitative configurations of discontinuities that can occur in the neighborhood of critical points. The second term in eqn. 3 does not contribute for discontinuities [10], and can be ignored in the analysis.

## 3- Problem formulation

### 3-1 System model

Consider a single generator supplying a P-Q load over a lossless transmission line as in figure 1 . The generator voltage is $v_1 = 1\, e^{j\delta}$, the load bus voltage $v_2 = V\, e^{j0}$ is taken as reference. The line admittance is $-jB$ (1 p u) and the load complex power demand is P+jQ (P>0 , Q>0) [11].

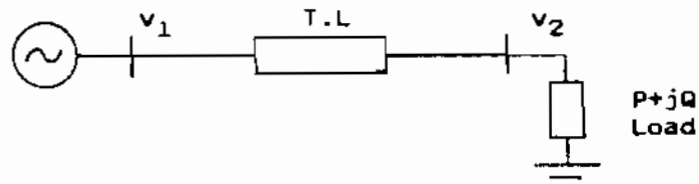


Figure 1: One generator supplying a P-Q load

The complex power injected into the network at the generator bus is

$$B\,v \sin\delta + j\,B(v^2 - v\cos\delta)$$

The complex power injected into the network at the load bus is

$$-B\,v\sin\delta - j\,B(v\cos\delta - v^2) = -P - jQ$$

which gives the power flow equations

$$0 = P - B\,v\sin\delta \qquad (4)$$
$$0 = Q - B\,v\cos\delta + Bv^2 \qquad (5)$$

The generator dynamics are given by the swing equation

$$M\ddot{\delta} = P_m - B\,v\sin\delta \qquad (6)$$

where,

$P_m$ is the input mechanical power.

To hold eqns. 4 and 5 in equilibrium, $P_m$ must equal $P$ and the system model becomes

$$M\ddot{\delta} = P - B\,v\sin\delta \qquad (7)$$
$$0 = Q - B\,v\cos\delta + B\,v^2 \qquad (8)$$

## 3-2 Construction of system energy function

The total system energy can be derived from equations 7 and 8

Multiplying both sides of eqn 7 by $w = o$ and integrating with respect to time, using as a lower limit $t = t_o$, where $\delta_o$ , $v_o$ are the initial stable equilibrium point, we obtain

$$\int M\dot{w}\,w\,dt = \int P\,\dot{\delta}\,dt - \int B\,v\sin\delta\,\dot{\delta}\,dt \qquad (9)$$

from eqn 8

$$\frac{Q}{v} = B\cos\delta - B\,v \qquad (10)$$

Multiplying both sides of eqn. 10 by $\dot{v}$, then eqn. 10 becomes

$$\frac{\dot{v}\, Q}{v} = B\,\dot{v}\cos\delta - B\,v\,\dot{v} \qquad (11)$$

where,

$$B\,\dot{v}\cos\delta = \frac{d(B\,v\cos\delta)}{dt} + B\,v\sin\delta\,\dot{\delta} \qquad (12)$$

Substituting eqn. 10 and 12 into eqn. 9, we obtain

$$\int_{\omega_o}^{\omega} M\,\dot{w}\,w\,dt = \int_{\delta_o}^{\delta} P\,d\delta + \int_{v_o,\delta_o}^{v,\delta} d(B\,v\cos\delta) - Q\int_{v_o}^{v} dv/v - \int_{v_o}^{v} B\,v\,dv \qquad (13)$$

$$M(w^2 - w_o^2)/2 = P(\delta - \delta_o) + B(v\cos\delta - v_o\cos\delta_o) - Q(\ln v - \ln v_o) - B(v^2 - v_o^2)/2 \qquad (14)$$

which gives an energy function such that

$$E(\delta,v) = M(w^2 - w_s^2)/2 - [\,P(\delta - \delta_s) + B(v\cos\delta - v_o\cos\delta_s) - Q(\ln v - \ln v_o) - B(v^2 - v_o^2)/2\,]$$

$$= E_K(w) + E_p(\delta,v) \qquad (15)$$

$E_K(w)$ is the system kinetic energy, and the $E_p(\delta,v)$ is the system potential energy.

where,

$$E_K(w) = M(w^2 - w_s^2)/2 \quad , \quad \text{and}$$

$$E_p(\delta,v) = -P(\delta - \delta_s) - B(v\cos\delta - v_o\cos\delta_o) + Q(\ln v - \ln v_s) + B(v^2 - v_o^2)/2$$

$$= -P\,\delta - B\,v\cos\delta + Q\ln v + B\,v^2/2 + K \qquad (16)$$

where,

$$K = P\,\delta_o + B\,v_o\cos\delta_o - Q\ln v_o - B\,v_o^2/2$$

In steady - state operation, the stored kinetic energy is too small and can be neglected, then eqn. 16 becomes

$$E(\delta,w)= E_p(\delta,v)= - P\,\delta - B\,v\cos\delta + Q\,\mathrm{Ln}\,v + 0.5\,B\,v^2 + K \qquad (17)$$

The equilibrium conditions for this system can be obtained by differentiating the above potential function with respect to state variables (angle and voltage) and equate them to zero. we get

$$\frac{\partial E_p(\delta,v)}{\partial \delta} = - P + B\,v\sin\delta = 0$$

then,

$$P = B\,v\sin\delta \qquad (18)$$

and

$$\frac{\partial E_p(\delta,v)}{\partial v} = - B\cos\delta + Q/v + B\,v$$

then,

$$Q = B\,v\cos\delta - B\,v^2 \qquad (19)$$

from 18 and 19, we obtain

$$[P/B\,v]^2 + [(Q + B\,v^2)/B\,v]^2 = 1 \qquad (20)$$

from which,

$$v^4 + v^2\,((2Q/B) - 1) + (Q^2 + P^2)/B^2 = 0 \qquad (21)$$

Let,

$$y = v$$
$$a = 2\,Q/B - 1$$
$$b = 0$$
$$c = (Q^2 + P^2)/B^2$$

then, eqn. 21 becomes

$$y^4 + a\,y^2 + b\,y + c = 0 \qquad (22)$$

Eqn. 22 is seen to be the swallowtail catastrophe manifold, with a control variable $b = 0$. The seven elementary catastrophes for the control space dimension less than or equal 4 have been well defined and explained [7-10]. The swallowtail catastrophe function used in this paper is shown in the appendix, then the equation is

$$(y^2)^2 + a\,(y^2) = 0 \qquad (23)$$

has the solution

$$y = [\ \pm\ (\ -a/2 \pm \sqrt{((a/2)^2 - c)})]^{1/2} \qquad (24)$$

Next, we find the singularity set, S, which is the subset of the catastrophe manifold (eqn. 22), that consists of all singular points corresponding to steady-state voltage instability. These are the points at which the first derivative of equation 23 equal to zero, as follows:

$$4\,y^3 + 2\,a\,y = 0$$

OR,

$$y = [\ -a/2\ ]^{1/2} \qquad (25)$$

It is clear that, the control parameter a should be less than zero and $0 < c < (a/2)^2$ to get the real solution.

The singularity set S is then projected down onto the control space to obtain the bifurcation set B . The bifurcation set is the image of catastrophe manifold in the control space. The bifurcation set B provides the region of all possible stable operations in terms of the control variables, which usually represent the system parameters. From eqns. 24 and 25 we obtain

$$c = (a/2)^2$$

therefore,

$$v_{crt} = (0.5 - Q/B)^{1/2} \qquad (26)$$

Equation 26 shows that, for stable operation at different values of reactive power, the system loading should satisfy the following equation

$$P < [ -Q B + (B/2)^2]^{1/2} \quad (27)$$

therefore, the maximum loading is

$$P_{max} = [- Q B + (B/2)^2]^{1/2}$$

As seen in this equation, the presence of a reactive component of load Q reduces the power limit. When reactive power compensation is used, to maintain voltage at load, the load power can be increased considerably. For example with purely shunt capacitor compensation, the maximum power is P = 0.707 as compared to P = 0.5 (at a voltage of 0.707) for no compensation. This is for load at unity power factor (purely active power). Typical values of critical load and critical voltage for different value of Q are given in table (1).

To increase the load power beyond these limits requires controlled compensation system. As one see that increasing capacitive reactive power increases the power limit and the critical voltage limit. But for higher values of compensation the normal voltage ranges may become critical

| system loading | catastrophe theory | | | critical voltage | system state |
|---|---|---|---|---|---|
| Q | $P_{max}$ | a | c | V | |
| 0.25 | 0.000 | -0.5 | 0.0625 | 0.5 | no |
| 0.5 $P_{max}$ | 0.309 | -0.69 | 0.1194 | 0.588 | compensation |
| 0.00 | 0.500 | -1.00 | 0.2500 | 0.707 | |
| -0.25 | 0.707 | -1.5 | 0.5625 | 0.866 | |
| -0.50 | 0.866 | -2.0 | 1.0000 | 1.000 | compensated |
| -0.75 | 1.000 | -2.5 | 1.5625 | 1.12 | |

Table (1)

## CONCLUSIONS

The mathematical method called catastrophe theory, previously applied to steady-state and transient synchronous stability of power systems. The analysis was with respect to angle instability. This paper explored the applicability of the theory to study steady-state voltage stability in terms of one of the elementary catastrophes Whilst an elementary example has been given, the approach is clearly capable of extension to study steady-state voltage stability in multimachine systems. This will be the subject of our next work.

## REFERENCES


1- MILLER,T.J.E, "Reactive power control in electric systems" John Wiley & Sons, New York, 1982.

2- GOOSSENS, J "Reactive power and system operation - incipient risk of generator constraints and voltage collapse", Proc. IFAC, Int. symp. on power systems and power plant control, seoul, Korea, August 1989, pp 3-12

3- SALLAM, A.A., and DINELEY, J.L.,"Catastrophe theory as a tool for determining synchronous power system dynamic stability", IEEE, Trans., 1983, PAS-102, pp 622-630

4- MAHMOUD, G.A, "Alternative method for assessing on-line transient stability", 25 th UPEC, Sept. 1990, pp 12-14, England.

5- WVONG, M.E, and MIHIRIG, A.M," Catastrophe theory applied to transient stability assessment of power systems", Proc.,IEE, vol. 133, Pt. c, No. 6,Sept.1986, pp 314-318.

6- CONCORDIA, C," Voltage instability", Electrical Power & Energy Systems Butterworth - Heinemann, May, 1989, pp 14-20

7- SAUNDERS, P.T., "An intrcduction to catastrophe theory" Cambridge University Press, Cambridge, 1980.

8- POSTON, T., and STEWART,I.," Catastrophe theory and applications", Pitman London, 1978.

9- ZEEMAN, E.C.,"Catastrophe theory", Scientific American April 1976, pp 65-83.

10- GILMORE, R.," Catastrophe theory for scientists and engineers", John Wiley & Sons, New York, 1981.

11- SHIGEO,ABE, and AKIRA,I,"Determination of power system voltage stability Part 3: Dynamical Approach", Proc.IEE Japan, vol. 103, No. 3, 1983, pp 57-65


## APPENDIX

The swallowtail catastrophe
The standard unfolding is

$$F(x;a,b,c) = x^5/5 + a\,x^3/3 + b\,x^2/2 + c\,x$$

and the catastrophe manifold M which is the surface of all

critical points is given by

$$DF_{a,b,c}(x) = 0 \quad (D \text{ denotes the derivative})$$

$$= x^4 + a\,x^2 + b\,x + c \qquad (28)$$

where x is the state variable and a, b and c are the control parameters. The critical points of degeneracy j are obtained by setting the first derivatives of F(x;a,b,c) equal to zero, as follows:

$$\text{twofold degenerate: } 4x^3 + 2ax + b = 0 \qquad (29)$$
$$\text{threefold degenerate: } 12x^2 + 2a = 0 \qquad (30)$$
$$\text{fourfold degenerate: } 24x = 0 \qquad (31)$$

From eqns 28-31, the function F(x;0,0,0) has fourfold degenerate critical points at x = 0. The curves of points in control parameter space which describe functions with threefold degenerate critical points (eqns. 28-30) with the parametric representation

$$a = -6x^2 \quad , \quad b = 8x^3, \quad c = -3x^4$$

these lines are shown in Fig. 2b.

The surface of points in control space which describe functions with twofold degenerate critical points, with the parametric representation (28-29)

$$b = -4x^3 - 2ax$$
$$c = 3x^4 + ax^2 \qquad (32)$$

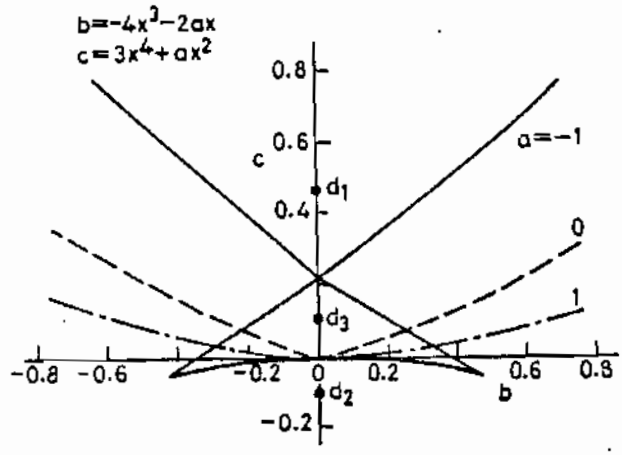


Figure 2a Three cross sections with a = positive, zero and negative value in 3-dimension space, computed by fixing a and letting x vary

By fixing the value of a in exprs. 32 and letting x vary, the three cross-sections of the surface at positive, zero and negative fixed values are computed as shown in Fig. 2a. These three cross-sections are pieced together by scaling to give the entire surface in the three dimensional space, as shown in Fig. 2b.

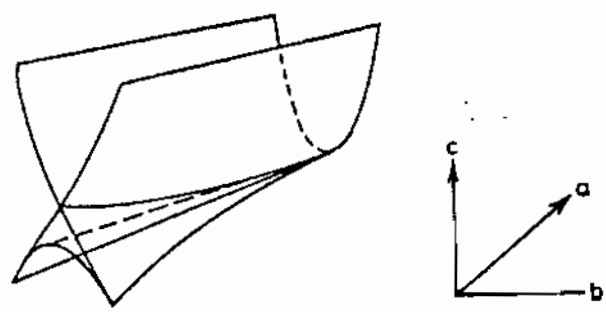


**Figure 2b Three cross sections shown in Figure 2a are joined together to construct swallowtail surface in 3-dimensional space**

This surface divides the three dimensional space into three open regions. The qualitative properties change as we pass through this surface. To determine the qualitative types of any region it is quite adequate to look at convenient points such as $d_1$, $d_2$, and $d_3$ in Fig. 2a, where b = 0; then the equation

$$(x^2)^2 + a\,x^2 + c = 0$$

has the solution

$$x = \sqrt{\pm\,( -a/2 + \quad [\,(a/2)^2 - c\,]^{0.5})}$$

For a > 0, there are no real solutions at c > 0
there are two real solutions at c < 0

For a < 0, there are no real solutions at $c > (a/2)^2$
two real solutions at c < 0
four real solutions at $0 < c < (a/2)^2$

# SWITCHED-RESISTOR LADDER FILTERS

## المرشحات السلميه باستخدام المقاومات المقطعه

By

M.A.ABO-Elsoud
Mansoura University
Mansoura, Egypt

T.ABD Elazim
Broadcasting&T .V
Union,CairoEgypt

الخلاصـــه :

يتناول هذا البحث أسلوب جديد لتصميم المرشحات السلميه ذات المقاومه المقطعـــه ويقوم هذه الطريقه على استبدال الملف او المكثف بأستخدام المكبل ذات المقاومه المقطعـــه بالاضافه الى استبدال المقاومه فى الدائره بمكبر تشغيل.

والغرض من هذا البحث هو تحويل المرشحات السلبيه ذات المكونات السلبيـه الى المكونات الايجابيه باستخدام تقنيه المقاومه المقطعه والتى يمكن تحقيقها بتكنولوجيا معدن اكسيـــــد شبه الموصـــل.

ABSTRACT

A systematic design technique for switched resistor (SR) ladder filter is described. The method is on the signal - flow graph (SFG) approach. Switched-resistor integrator using a modified SR MOSFET is investigated. This integrator achieves MOS nonlinearity cancellation and does not require the use of fully balanced op amps. It is used to simulate either inductor or capacitor. Design and experimental results are given for a fifth-order low filter.

## I. INTRODUCTION

The simulation of passive doubly terminated ladder filters has been used extensively in the past few years for the design of active and digital filters. Because of their low sensitivity properties, active ladder filters are used to simulate LC filters. There are two classes of RC-active filters that simulate LC filters. The first class uses direct immitance simulation and the concepts of the immitance conversion [1]. The second class of circuit uses inverting and noninverting integrator to simulate the SFG [6].

Several approaches for switched capacitor (SC) ladder filters have been discussed [2],[3]. In this technique, any SC network requires to operate with two phase nonoverlapping clocks. Moreover, the [illegible] SC products are determined by capacitor

The purpose of this paper is to give a simple step-by-step design procedure for a new SFG filters. A new SR integrator using two analog MOS switches as a linear resistor is described. This integrator can be simulated either by the admittance of inductor or by the impedance of capacitor. High order SR low-pass filter is implemented. This filter achieves low sensitivity to the components, better temperature stability.

## II. NEW SWITCHED RESISTOR INTEGRATORS

In the SFG, the basic element is op amp integrator. The conventional integrator is shown in Fig.1 (a). Its transfer function is given by :

$$H(s) = -1/sRC \qquad (1)$$

Where the integrator bandwidth is 1/RC

A switched resistor version of this integrator is shown in Fig.2.(b), in which the resistor R has been replaced by two MOSFETS using the control signal as shown in fig.2.

It is well known that the drain current $I_D$ of MOSFET in the triode region is given by :

$$I_D = K\,[(V_{GS}-V_T)V_{DS}-V_{DS}^2/2] \qquad (2)$$

Where $K = C_o \cdot \mu \cdot W/L$, and $C_o$ is oxide capacitance, $\mu$ is the effective mobility of the channel carrier, W the channel width, and L the channel length.

$$I_{D1} = K\,[(V_G - V_T)V_{1,2} - V_{1,2}^2/2] \qquad (3)$$

$$I_{D2} = K\,[(V_{1,2} - V_T)V_{1,2} - V_{1,2}^2/2] \qquad (4)$$

Then the total current $I_t$ is

$$I_t = I_{D1} + I_{D2} = K(V_G - 2V_T)\, V_{12} \qquad (5)$$

From equation (5), it is noted that the nonlinear term $V_{DS}^2/2$ in the two MOSFETS is cancelled. For the usual case of $V_{DS}-V_T >> V_{DS}$ , then the equivalent resistance between terminals 1 and 2 is given by

$$R = 1/[k(V_G - 2V_T)] \qquad (6)$$

During the time the switch is off, or during the turn-on and turn off transients [7], the equivalent resistance in Fig.1(b) is given by [4]

$$R_s = R_{ON}\,(T/\tau) \qquad (7)$$

Where $R_{ON}$ is the total on - resistance of the two MOS switches.

The transfer function of the SR integrator in Fig.1(b) is

$$H(S) = -1/sR_sC \qquad (8)$$

The bandwidth of the SR integrator is $\dfrac{1}{R_{ON}C}$ $(\tau/T)$

Fig.3 represents the SR inverting lossy integrator. Its transfer function is given by :

$$H(s) = -\frac{R_2/R_1}{s+1/R_2C} \qquad (9)$$

## III. DESIGN OF ACTIVE LADDER FILTERS

In this section, a SFG method will be presented for transforming a passive doubly terminated networks into active ladder equivalents using switched resistors integrators.

It is known that a passive doubly terminated RLC in Fig.4 achieves very low sensitivity to component variations in passband response. Fig.4 shows doubly terminated fifth - order low-pass filter. The branch relationships describing the ladder are

$$I_1 = \left(\frac{1}{R_1 + sL_1}\right)(V_{in} - V_2) \tag{10}$$

$$= Y_1 (V_{in} - V_2)$$

$$V_2 = \frac{1}{sC}(I_1 - I_3)$$

$$= Z_2 (I_1 - I_3) \tag{11}$$

$$I_3 = \left(\frac{1}{sL_3}\right)(V_2 - V_4)$$

$$= Y_3 (V_2 - V_4) \tag{12}$$

$$V_4 = \left(\frac{1}{sC_4}\right)(I_3 - I_5)$$

$$= Z_4 (I_3 - I_5) \tag{13}$$

$$I_5 = \frac{V_4}{R_2 + sL_5}$$

$$= Y_5 . V_4 \qquad (14)$$

$$V_o = R_2 \; I_5 \qquad (15)$$

The flow diagram represents the equations above as shown in Fig.5. The admittance $Y_1$ and $Y_4$ can be realized by the SR inverting lossy integrator of Fig.3. Finaily, the impedances $Z_2$, $Z_4$ and the admittance $Y_3$ can be realized by the SR inverting integrator of Fig.1(b). One can take advantage of the fact that $R_1 = R_2 = 1$ ohm.

Accordingly, the fifth order low pass filter in Fig.4 can be implemented using the circuits shown in fig.1(b) and 3, and unity gain inverters. Fig.6 shows the new SR filter circuit. The capacitors of the SR integrators of Fig.6 are calculated from the following equation obtained by solving Eqs. (8), (9) and Eqs. 10 to 15 :

$$C_{L1} = L_1 \; R_4 \qquad (16)$$

$$C_{C2} = C_2 \cdot R_4 \qquad (17)$$

$$C_{L3} = L_3 \; R_4 \qquad (18)$$

$$C_{L4} = C_4 / R_4 \qquad (19)$$

$$C_{L5} = L_5 \; R_4 \qquad (20)$$

Assuming $R = R_{min}$ (Ω) with any value of interest and applying the equation above, we get the capacitor value of the SR integrators of Fig.6.

## IV. EXPERIMENTAL RESULTS

An SR active fifth - order low pass ladder filter derived from the RLC prototype of Fig.4 has been implemented using modified SR integrator. The filter was built employing discrete components. All op amps used in Fig.6 were MOS op amps. D-MOS switched of the SD 5000 having low feedthrough were also used.

The proposed filter was designed for a cutoff frequency of 1500 hz with sampling rate 100 khz. The frequency response of the filter is shown in fig.7.

## CONCLUSION

A systematic design for switched- resistor ladder filter is presented. A modified SR integrator having MOS nonlinearity cancellation has been discussed. SR high - order ladder filters can be realized with transfer functions that are insensitive to component variations. Moreover, these filters achieve better stability temperature using MOS technology.

## REFERENCES

[1] L.T.Bruton "Multipe Amplifier RC-Active Filter Design with Emphasis on GIC Realizations", IEEE Trans. Circuits Sys.,vol. CAS-25, PP.830-845, Oct.1978.

[2] G.M.Jacobs et al,"Design Techniques for MOS Switched. Capacitor Ladder Filters",IEEE Trans. Circuit Sys.,vol. CAS-25 PP 1014-1021,Dec.1978.

[3] D.J.Allstot et al, "MOS Switched capacitor Ladder Filters",IEEE J.Solid-State Circuits,Vol SC-13,PP.805-814,DEC.1978

[4] M.A.Abo-Elsoud and J.C. Mtheou,"Analysis of Switched Resistor Circuits,Proc. of the 4th national radio science Symposium,nov.,1986.

[5] M.A.Abo-Elsoud,"Switched-Resistor Filters using Unity Gain Amplifier,Proc. of the 31st Midwest Symposium on Circuits and System Au Aug.1988.88.

[6] K.Martin and A.S.Sedra ,"Design of signal-flow Graph (SFG) actiralirit ," ,"IETraTranCirCircuSysSyst,Vol.cal CAS-25, IP.185-195,Apr.1978.

[7] R.Gregorian and G.C.Temes, "Analog MOS integrated Circuit for SignalProcessing ,Wiley-Interscience,1986p84

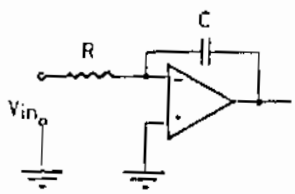


( a )

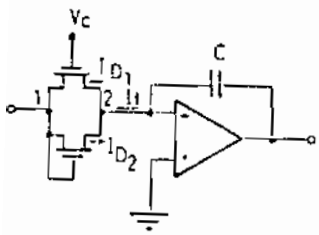


Fig. 1 ( b )

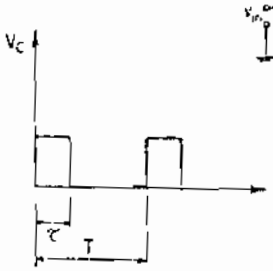


Fig 2

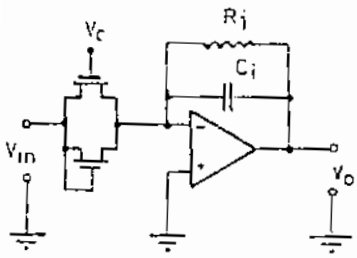


Fig 3

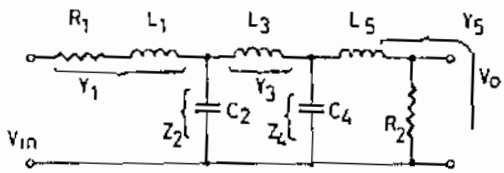


Fig. 4

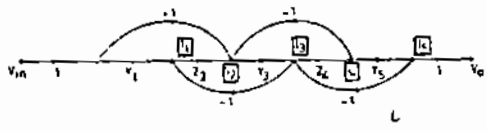

Fig 5

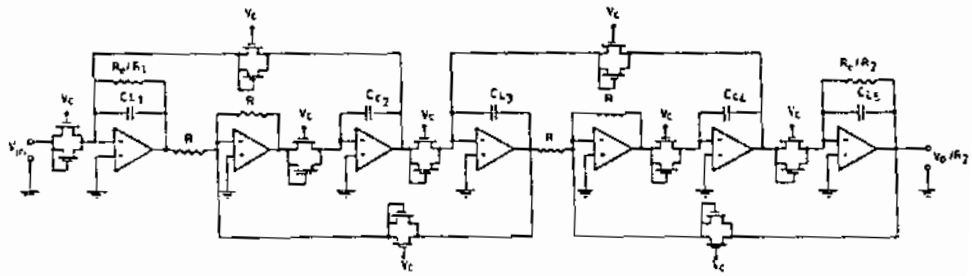

Fig 6

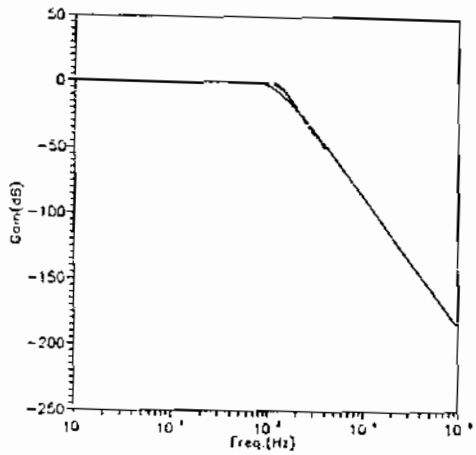


Fig 7. Fifth Order Leapfrog Low-pass Filter At Duty Cycle 21%